Knockdown of the type 2 and 3 inositol 1,4,5-trisphosphate receptors suppresses muscarinic antinociception in mice.

Neuroscience 149 (2007) 409–420

KNOCKDOWN OF THE TYPE 2 AND 3 INOSITOL 1,4,5-TRISPHOSPHATE RECEPTORS SUPPRESSES MUSCARINIC ANTINOCICEPTION IN MICE

N. GALEOTTI,[a]* A. QUATTRONE,[b] E. VIVOLI,[a] A. BARTOLINI[a] AND C. GHELARDINI[a]

[a]*Department of Preclinical and Clinical Pharmacology, University of Florence, Viale G. Pieraccini 6, I-50139 Florence, Italy*

[b]*Laboratory of Magnetic Resonance Center and FiorGen Foundation, University of Florence, Via Sacconi 6, 50019 Florence, Italy*

Abstract—The involvement of central endoplasmic inositol 1,4,5-trisphosphate receptors (IP_3R) in muscarinic antinociception was investigated in the mouse hot plate test. Selective knockdown of type 1, 2 and 3 IP_3R was obtained by means of an antisense oligonucleotide (aODN) strategy. A selective IP_3R protein level reduction of approximately 30–50% produced by aODN administration for each receptor subtype investigated was demonstrated by Western blotting experiments. I.c.v. pretreatment with an aODN complementary to the sequence of the type 2 IP_3R (0.1–3 nmol per mouse i.c.v.) prevented the antinociception induced by physostigmine (0.15 mg kg^{-1} s.c.) and oxotremorine (60 μg kg^{-1} s.c.). Similarly, an aODN against type 3 IP_3R (0.1–3 nmol per mouse i.c.v.) antagonized cholinergic antinociception. A shift to the right of the physostigmine dose–response curve was obtained after anti-type 2 IP_3R2 and anti-type 3 IP_3R treatments. Conversely, pretreatment with an aODN complementary to the sequence of type 1 IP_3R (0.1–5 nmol per mouse i.c.v.) did not modify the antinociception induced by physostigmine and oxotremorine. Mice undergoing treatment with aODNs did not show any impairment of the locomotor activity, spontaneous motility and exploratory activity as revealed by the rota-rod and hole board tests. These results indicate a selective involvement of type 2 and 3 IP_3R in central muscarinic antinociception in mice.

Key words: muscarinic receptor, antinociception, type 1 inositol-1,4,5-trisphosphate receptors, type 2 inositol-1,4,5-trisphosphate receptors, type 3 inositol-1,4,5-trisphosphate receptors, intracellular Ca^{2+}

Several literature reports indicate that supraspinal cholinergic antinociception induced both directly, through muscarinic agonists, and indirectly, by enhancing ACh extracellular levels through cholinesterase inhibitors, is mediated by M_1 receptor stimulation, indicating that M_1 muscarinic receptor subtype plays an essential role in the modulation of pain perception (Bartolini et al., 1992; Iwamoto and Marion, 1993; Ghelardini et al., 1996; Naguib and Yaksh, 1997; Ghelardini et al., 2000). More recently, intracellular mechanisms involved in supraspinal muscarinic antinociception in a condition of acute thermal nociception in normal animals have been investigated. M_1 muscarinic receptors typically couple via the α subunits of the $G_{q/11}$ family to activate phospholipase C (PLC) (Caulfield and Birdsall, 1998), and the activation of PLC results in hydrolysis of phosphatidyl 4,5-bisphosphate and production of inositol-1,4,5 trisphosphate (IP_3) and diacylglycerol (DAG). The main effect of DAG is to activate protein kinase C; IP_3 mediates the release of calcium from intracellular stores by binding to its receptors (Berridge, 1993). The involvement of receptor-mediated activation of the PLC–IP_3 pathway in the increase in pain threshold produced by administration of cholinomimetics was directly demonstrated. The inhibition of the IP_3 synthesis by pretreatment with LiCl, and the blockade of IP_3 receptors (IP_3R) by administration of the IP_3R antagonist heparin, dose dependently prevented physostigmine and oxotremorine antinociception (Galeotti et al., 2003).

The receptor that recognizes IP_3 was first characterized as a protein called P400 that was enriched in normal cerebella (Mikoshiba et al., 1997); two other types of IP_3 receptors were then cloned. The original IP_3 receptor was named type 1 IP_3 receptor (IP_3R1), whereas the others were named type 2 IP_3 receptor (IP_3R2) and type 3 IP_3 receptor (IP_3R3) (Patel et al., 1999). IP_3Rs are recognized as a protein family of tetrameric ligand-gated Ca^{2+} channels that allow mobilization of intracellular Ca^{2+} stores in response to activation of cell surface receptors linked to IP_3 generation (Berridge, 1993). IP_3R monomers are large proteins with a calculated molecular mass of about 300 kDa and all three isoforms of IP_3R share 60–70% amino acid similarity (Taylor et al., 1999).

The aim of the present study was to investigate the role of type 1, 2 and 3 IP_3Rs in the intracellular mechanism of muscarinic antinociception at a supraspinal level. To this purpose, we inhibited the expression of each IP_3 receptor subtype by using antisense oligonucleotides targeting IP_3R mRNA sequences that are unique in the mouse genome and therefore assured stringent target selectivity.

*Corresponding author. Tel: +39 055 4271312; fax: +39 055 4271280.
E-mail address: nicoletta.galeotti@unifi.it (N. Galeotti).

Abbreviations: aODN, antisense oligonucleotide; CNS, central nervous system; DAG, diacylglycerol; dODN, degenerate oligonucleotide; IP_3R1, type 1 inositol-1,4,5-trisphosphate receptors; IP_3R2, type 2 inositol-1,4,5-trisphosphate receptors; IP_3R3, type 3 inositol-1,4,5-trisphosphate receptors; PAGE, polyacrylamide gel electrophoresis; PBST, phosphate-buffered saline containing 0.1% Tween; PLC, phospholipase C; SDS, sodium dodecyl sulfate.

0306-4522/07$30.00+0.00
doi:10.1016/j.neuroscience.2007.07.049

EXPERIMENTAL PROCEDURES

Animals

Male Swiss albino mice (24–26 g) from Morini (San Polo d'Enza, Italy) were used. Fifteen mice were housed per cage. The cages were placed in the experimental room 24 h before the test for acclimatization. The animals were fed a standard laboratory diet and tap water *ad libitum* and kept at 23±1 °C with a 12-h light/dark cycle, light at 7 AM. All experiments were carried out in accordance with the European Communities Council Directive of 24 November 1986 (86/609/EEC) for experimental animal care. All efforts were made to minimize the number of animals used and their suffering.

Hot plate test

Mice were placed inside a stainless-steel container, which was set thermostatically at 52.5±0.1 °C in a precision water bath from KW Mechanical Workshop (Siena, Italy). Reaction times (in seconds) were measured with a stopwatch before and 15, 30, 45 and 60 min after administration of the analgesic drug. The endpoint used was the licking of the fore or hind paws. Those mice scoring less than 12 and more than 18 s in the pretest were rejected (30%). An arbitrary cutoff time of 45 s was adopted. The observers were unaware of the treatments. A total of 12–15 mice per group were tested.

Rota-rod test

The apparatus consisted of a base platform and a rotating rod with a diameter of 3 cm and a nonslippery surface. The rod was placed at a height of 15 cm from the base. The rod, 30 cm in length, was divided into five equal sections by six disks. Thus, up to five mice were tested simultaneously on the apparatus, with a rod-rotating speed of 16 rpm. The integrity of motor coordination was assessed on the basis of the number of falls from the rod in 30 s according to Vaught et al. (1985). Those mice scoring less than three and more than six falls in the pretest were rejected (20%). The performance time was measured before (pretest) and 15, 30 and 45 min after the beginning of the test. A total of 12–15 mice per group were tested.

Hole board test

The hole board test consisted of a 40-cm^2 plane with 16 flush-mounted cylindrical holes (3 cm diameter) distributed four by four in an equidistant, grid-like manner. Mice were placed on the center of the board one by one and allowed to move about freely for a period of 5 min each. Two electric eyes, crossing the plane from midpoint to midpoint of opposite sides, thus dividing the plane into four equal quadrants, automatically signaled the movement of the animal (counts in 5 min) on the surface of the plane (spontaneous motility). Miniature photoelectric cells in each of the 16 holes recorded (counts in 5 min) the exploration of the holes (exploratory activity) by the mice. A total of 12–15 mice per group were tested.

I.c.v. injection technique

I.c.v. administration was performed under ether anesthesia with isotonic saline as solvent, as previously described (Galeotti et al., 2003). Briefly, during anesthesia, mice were grasped firmly by the loose skin behind the head. A hypodermic needle (0.4 mm external diameter) attached to a 10-μl syringe was inserted perpendicularly through the skull and no more than 2 mm into the brain of the mouse, where 5 μl solution was then administered. The injection site was 1 mm to the right or left from the midpoint on a line drawn through to the anterior base of the ears. Injections were performed randomly into the right or left ventricle. To ascertain that solutions were administered exactly into the cerebral ventricle, some mice were injected with 5 μl of diluted 1:10 India ink and their brains were examined macroscopically after sectioning. The accuracy of the injection technique was evaluated with 95% of injections being correct.

Drugs

The following drugs were used: physostigmine hemisulphate, oxotremorine methiodide (Sigma, Milan, Italy), and D-amphetamine (De Angeli, Rome, Italy). Other chemicals were of the highest quality commercially available. Drugs were dissolved in isotonic (NaCl 0.9%) saline solution immediately before use. Drug concentrations were prepared so that the necessary dose could be administered in a volume of 10 ml kg^{-1} by s.c. injection. Physostigmine was administered at a dose of 0.15 mg/kg, whereas oxotremorine was injected at a dose of 60 μg/kg.

Antisense oligonucleotides

Phosphodiester oligonucleotides (ODNs) protected by terminal phosphorothioate double substitution (capped ODNs) against exonuclease-mediated degradation were purchased from Tib-Molbiol (Genoa, Italy). The sequences were as follows: anti-IP_3R1, 5′-C*T*C GAC ATT TTG TCA GAC* A*T-3′, targeting the mRNA (GenBank NM_010585.2) at positions 329–348; anti-IP_3R2, 5′-A*G*G AAG CTG GAC ATT TTG* T*C-3′ targeting the mRNA (GenBank NM_019923.3) at positions 41–60; anti- –IP_3R3, 5′-C*T*G GAC ATT TCA TTC ATG* G*C-3′ targeting the mRNA (GenBank NM_080553.2) at positions 48–67 (* indicates phosphorothioate residues). A 20-mer fully degenerated ODN (dODN) 5′-N*N*N NNN NNN NNN NNN* N*N-3′ (where N is G, C, A or T) was used as a control ODN.ODNs were vehiculated intracellularly by an artificial cationic lipid (DOTAP, Sigma, Milan, Italy) to enhance both uptake and stability. aODNs or dODNs were preincubated at 37 °C for 30 min with 13 μM DOTAP and supplied to mice by i.c.v. injection of 5 μl solution on days 1, 2 and 3. Behavioral tests were performed on day 4, 24 h after the last i.c.v. injection of ODNs. Doses and administration schedule of aODNs were chosen on the bases of time-course and dose–response experiments performed in our laboratory.

Preparation of membranes

Mouse brains were dissected to separate specific areas. Mouse cerebellum, hippocampus, cortex and striatum were homogenized in a homogenization buffer containing 25 mM Tris–HCl, pH 7.5, 25 mM NaCl, 5 mM EGTA, 2.5 mM EDTA, 2 mM NaPP, 4 mM PNFF, 1 mM Na_3VO_4, 1 mM phenylmethylsulfonyl fluoride (PMSF), 20 μg/ml leupeptin, 50 μg/ml aprotinin, and 0.1% sodium dodecyl sulfate (SDS). The homogenate was centrifuged at 9,000×g for 15 min at 4 °C and the low-speed pellet was discarded. The microsomal membranes were obtained from the supernatant of the 9,000×g spin by centrifugation at 100,000×g for 1 h at 4 °C. Microsomes were resuspended in homogenization buffer and stored at −80 °C. Protein concentration of the microsomal fraction was quantified using a protein assay kit (Bio-Rad Laboratories, Milan, Italy).

Western blot analysis

Membrane homogenates (30 μg) made from cerebellum, hippocampus, cortex and striatum regions of control and antisense-treated mice were separated on 6% SDS–polyacrylamide gel electrophoresis (PAGE) and transferred onto nitrocellulose membranes (60 min at 100 V) using standard procedures. Membranes were blocked in PBST (phosphate-buffered saline containing 0.1% Tween) containing 5% nonfat dry milk for 90 min. Following washings, blots were incubated overnight at 4 °C with specific antibodies (Santa Cruz Biotechnology, Santa Cruz, CA, USA) against IP_3R1, IP_3R2, IP_3R3 or β-actin (1:1000 dilution). After

being washed with PBST, the nitrocellulose membrane was incubated with rabbit anti-goat horseradish peroxidase-conjugated secondary antisera (1:10,000) and left for 1 h at room temperature. Blots were then extensively washed according to the manufacturer's instruction and developed using an enhanced chemiluminescence detection system (Pierce, Milan, Italy). Exposition and developing time were standardized for all blots. Densitometric analysis of scanned images was performed on a Macintosh iMac computer (Apple Computer, Inc., Cupertino, CA, USA) using the public domain NIH Image program. Measurements in control samples were assigned a relative value of 100%.

Immunoprecipitation of IP_3R1, IP_3R2, IP_3R3

Immunoprecipitation was carried out on 1 ml of microsomal fraction containing 100 μg proteins by incubation for 2 h at 4 °C with 10 μg of specific antibody against IP_3R1, IP_3R2 or IP_3R3. All tubes then received 20 μl of 25% (v/v) Protein G–agarose (Santa Cruz Biotechnology) and incubated for a further 2 h at 4 °C. Pellets were collected by centrifugation at 1,000×*g* for 5 min at 4 °C and washed three times with homogenization buffer. Pellets were finally resuspended in 40 μl electrophoresis sample buffer and boiled for 5 min, and samples were processed by SDS–PAGE.

Statistical analysis

All experimental results are given as the mean±SEM. An analysis of variance (ANOVA), followed by Fisher's protected least significant difference procedure for post hoc comparison, was used to verify significance between two means. Data were analyzed with the StatView software for the Macintosh computer. *P* values of less than 0.05 were considered significant.

RESULTS

Effect of anti-IP_3R1, anti-IP_3R2, and anti-IP_3R3 on mouse pain threshold

Pretreatment with an aODN against IP_3R1 (3–5 nmol per mouse per i.c.v. injection) did not produce any modification of the mouse pain threshold by comparing licking latency values obtained before the beginning of the i.c.v. treatment and 24 h after the end of the treatment. Similar results were obtained with administration of an aODN against IP_3R2 (3 nmol per mouse per i.c.v.) and of an aODN against IP_3R3 (3 nmol per mouse per i.c.v.). Comparing the dODN- and aODN-treated mice, no difference among the licking latency values was observed (Fig. 1). Higher doses of anti-IP_3R2 and anti-IP_3R3 were not investigated due to the toxicity induced.

dODN pretreatment did not modify the mouse pain threshold in comparison with DOTAP- and saline-treated animals and with naive animals (data not shown).

Role of IP_3R1, IP_3R2, and IP_3R3 on muscarinic antinociception

Pretreatment with an aODN against IP_3R1 (0.1–5 nmol per mouse per i.c.v. injection) did not modify the antinociceptive effect produced by physostigmine (0.15 mg kg^{-1} s.c.) and oxotremorine (60 μg kg^{-1} s.c.) administration (Fig. 2). In contrast, knockdown of IP_3R2 (0.1–3 nmol per mouse per i.c.v.injection) prevented the physostigmine- and ox-

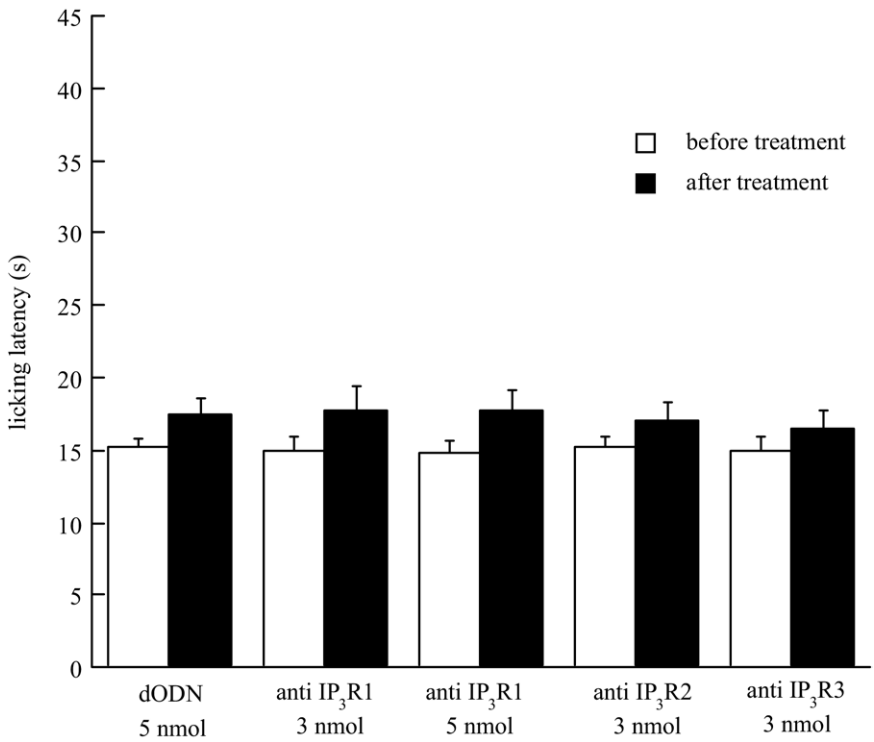

Fig. 1. Effect of pretreatment with anti-IP_3R1 (3–5 nmol per mouse i.c.v.), anti-IP_3R2 (3 nmol per mouse i.c.v.) and anti-IP_3R3 (3 nmol per mouse i.c.v.) on the mouse pain threshold evaluated in the mouse hot plate test. The licking latency values were recorded 24 h after the end of the ODNs treatments. Vertical lines represent S.E.M.

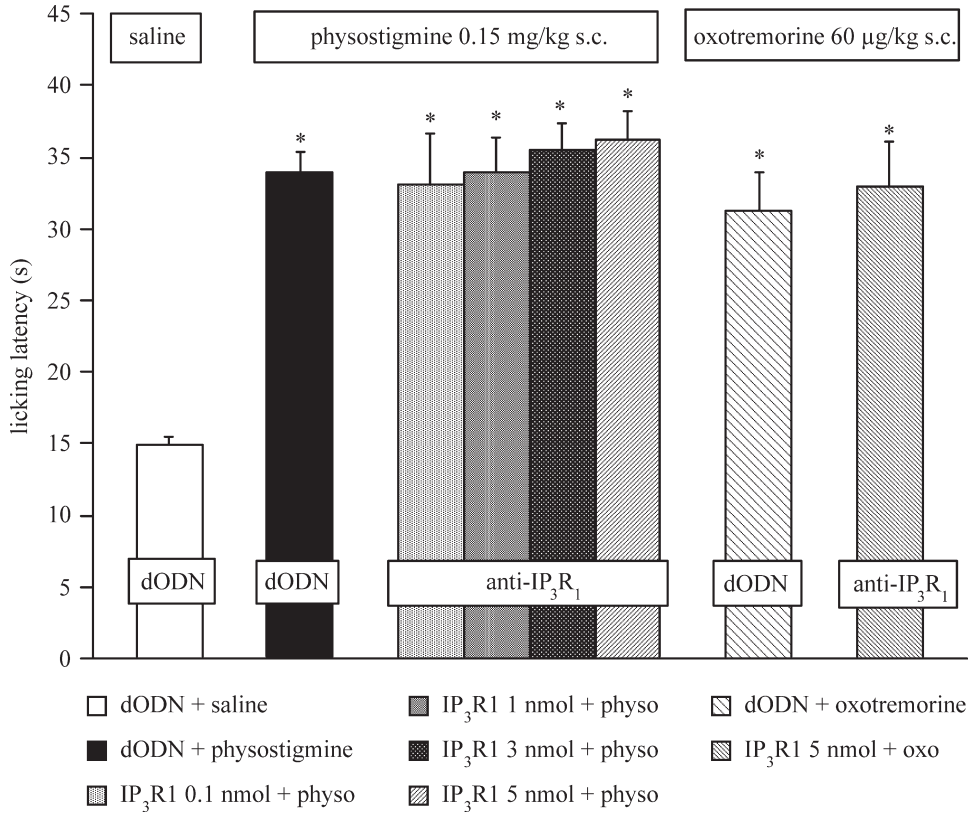

Fig. 2. Lack of effect of anti-IP_3R1 treatment (0.1–5 nmol per mouse i.c.v.) on physostigmine (0.15 mg kg^{-1} s.c.)- and oxotremorine (60 μg kg^{-1} s.c.)-induced antinociception in the mouse hot plate test. The licking latency values were recorded 30 min after cholinomimetic administration. ODNs were administered 72, 48 and 24 h prior to the behavioral tests. Vertical lines represent S.E.M. * $P<0.001$ in comparison with control group (dODN+saline-treated mice).

otremorine-induced increase of pain threshold in comparison with dODN-treated mice (Fig. 3A). A shift to the right of the dose–response curve of physostigmine (Fig. 3B) and oxotremorine (Fig. 3C) after anti-IP_3R2 pretreatment was observed. Similar results were obtained with anti-IP_3R3 pretreatment. Administration of an aODN against IP_3R3 (0.1–3 nmol per mouse per i.c.v. injection) prevented physostigmine and oxotremorine antinociception (Fig. 4A). aODN pretreatment shifted the dose–response curve of physostigmine (Fig. 4B) and oxotremorine (Fig. 4C) to the right. The antagonistic effect on physostigmine antinociception produced by the anti-IP_3R2 and anti-IP_3R3 treatments disappeared 7 days after the end of the treatment.

dODN pretreatment did not modify the mouse sensitivity to the physostigmine and oxotremorine antinociceptive effect in comparison with naive, DOTAP- and saline-treated mice (data not shown).

Effect of treatments on mouse motor coordination and spontaneous motility

The aODN, at the highest effective doses, were tested in order to assess their effect on mouse behavior. Mice pretreated with anti-IP_3R1 (5 nmol per mouse i.c.v.), anti-IP_3R2 (3 nmol per mouse i.c.v.), anti-IP_3R3 (3 nmol per mouse i.c.v.) and dODN (5 nmol per mouse i.c.v.) were evaluated for motor coordination by use of the rota-rod test and for spontaneous mobility and inspection activity by use of the hole board test. The endurance time, evaluated before and 15, 30 and 45 min after the beginning of the rota-rod test, demonstrated the lack of any impairment in the motor coordination of animals pretreated with aODNs in comparison with the dODN group (Fig. 5A). The spontaneous mobility as well as the inspection activity of mice, expressed as counts in 10 min, was unmodified by pretreatment with aODNs in comparison with the dODN group. D-Amphetamine, used as positive control, significantly increased both parameters evaluated (Fig. 5B). Higher doses of the aODNs employed were not investigated because they induced behavioral side effects such as tremors and convulsions or death.

Effect of aODNs on IP_3R1, IP_3R2 and IP_3R3 protein levels

Mice were treated with the aODNs on days 1, 2 and 3. On day 4, 24 h after the last i.c.v. injection, mice were killed and the cerebellum, cortex, striatum and hippocampus were dissected and examined for the levels of expression of IP_3R1, IP_3R2 and IP_3R3 in comparison with mice treated with dODN. Figure 6A shows a representative immunoblot where a prominent approximately 260-kDa protein band was observed, indicating that all three receptor subtypes

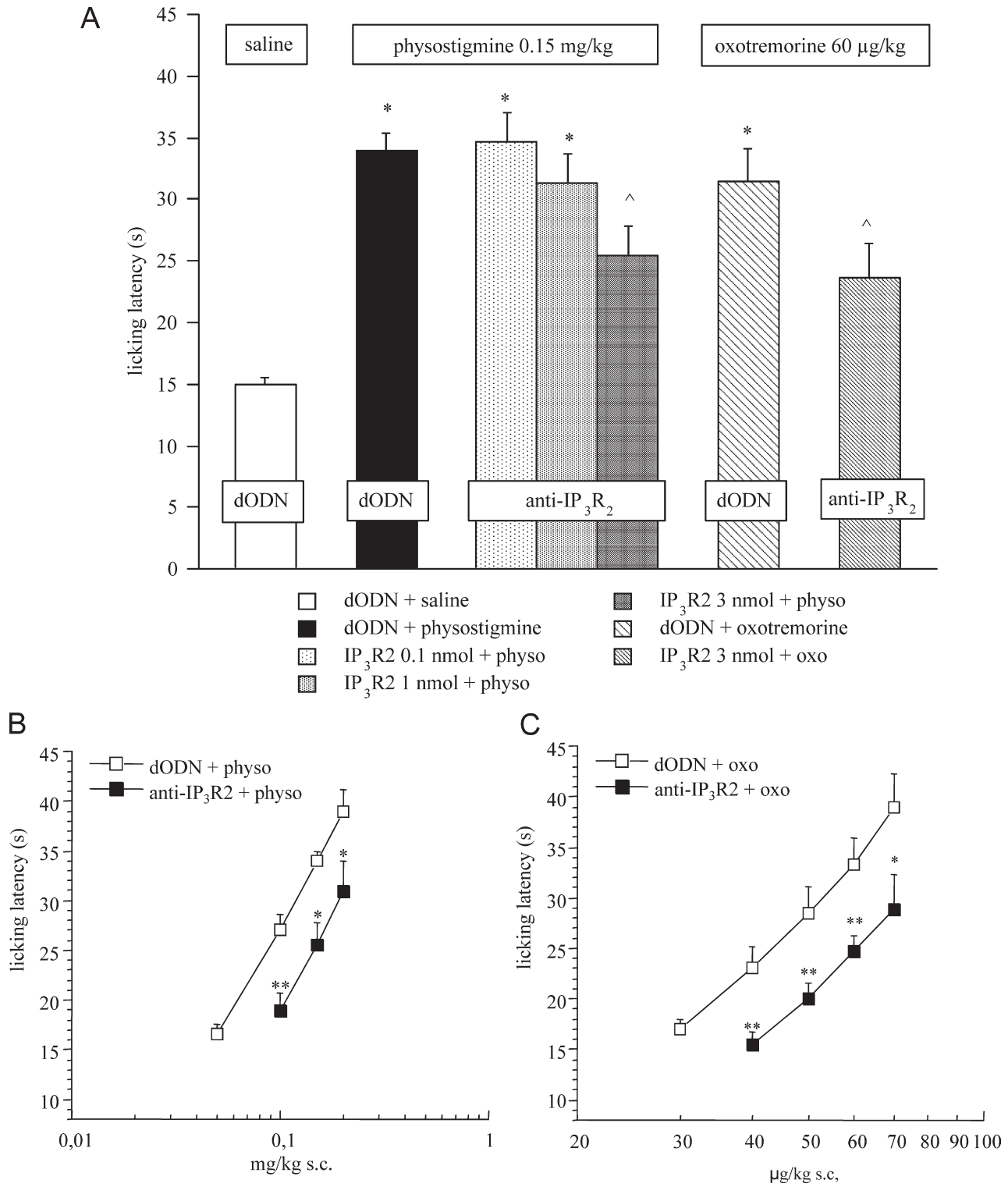

Fig. 3. (A) Prevention by an anti-IP_3R2 treatment (0.1–3 nmol per mouse i.c.v.) of physostigmine (0.15 mg kg^{-1} s.c.) and oxotremorine (60 μg kg^{-1} s.c.)-induced antinociception in the mouse hot plate test. The licking latency values were recorded 30 min after cholinomimetic administration. ODNs were administered 72, 48 and 24 h prior to the behavioral tests. Vertical lines represent S.E.M. * $P<0.001$ in comparison with control group (dODN+saline-treated mice); ^ $P<0.05$ in comparison with dODN+cholinomimetic-treated mice. (B) Shift to the right of the physostigmine dose–response curve by pretreatment with anti-IP_3R2 3 nmol per mouse i.c.v. Vertical lines represent S.E.M. * $P<0.05$, ** $P<0.01$ in comparison with dODN+ physostigmine-treated mice. (C) Shift to the right of the oxotremorine dose–response curve by pretreatment with anti-IP_3R2 3 nmol per mouse i.c.v. Vertical lines represent S.E.M. * $P<0.05$, ** $P<0.01$ in comparison with dODN+oxotremorine-treated mice.

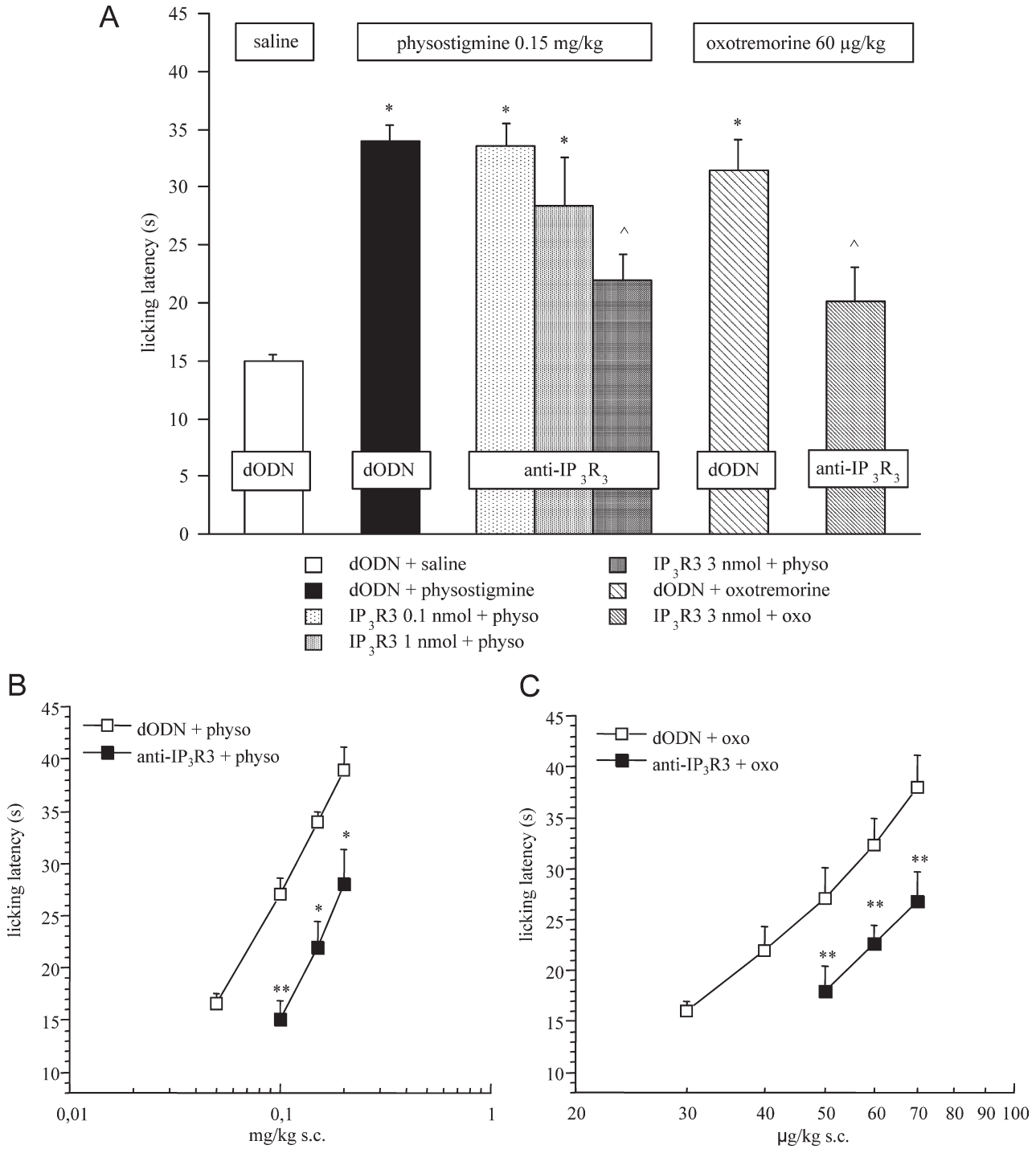

Fig. 4. (A) Prevention by an anti-IP_3R3 treatment (0.1–3 nmol per mouse i.c.v.) of physostigmine (0.15 mg kg^{-1} s.c.) and oxotremorine (60 μg kg^{-1} s.c.)-induced antinociception in the mouse hot plate test. The licking latency values were recorded 30 min after cholinomimetic administration. ODNs were administered 72, 48 and 24 h prior to the behavioral tests. Vertical lines represent standard error of the mean. * $P<0.001$ in comparison with control group (dODN+saline-treated mice); ^ $P<0.05$ in comparison with dODN+cholinomimetic-treated mice. (B) Shift to the right of the physostigmine dose–response curve by pretreatment with anti-IP_3R3 3 nmol per mouse i.c.v. Vertical lines represent S.E.M. * $P<0.05$, ** $P<0.01$ in comparison with dODN+physostigmine-treated mice. (C) Shift to the right of the oxotremorine dose–response curve by pretreatment with anti-IP_3R3 3 nmol per mouse i.c.v. Vertical lines represent S.E.M. ** $P<0.01$ in comparison with dODN+oxotremorine-treated mice.

were expressed in the above-mentioned cerebral areas. The dODN did not significantly change the level of immunostaining when compared with that of naive animals (data not shown). A statistically significant reduction of the expression of IP_3R1, IP_3R2 and IP_3R3 after aODN treatment in comparison with mice treated with the corresponding

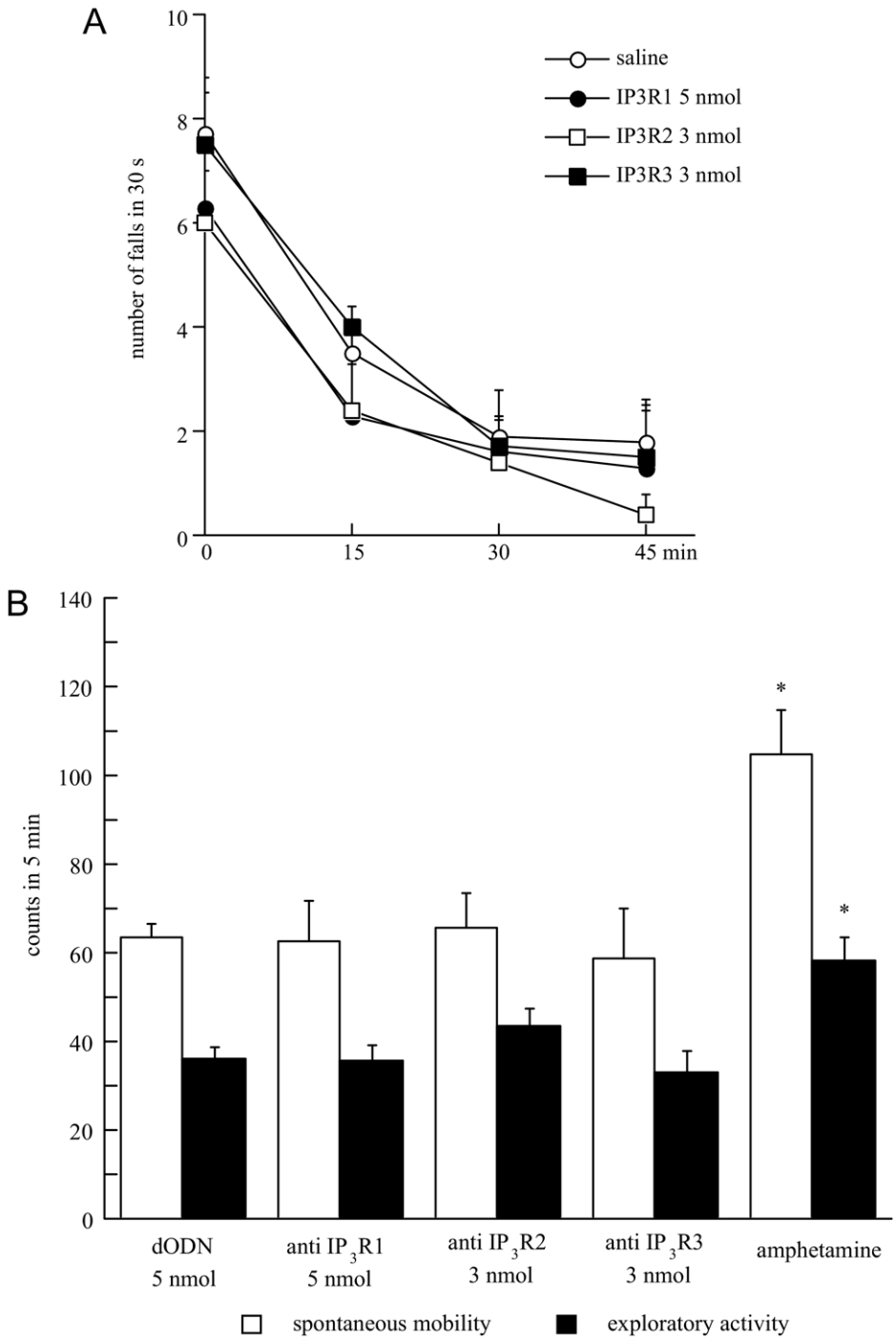

Fig. 5. (A) Lack of effect of anti-IP_3R1 (5 nmol per mouse i.c.v.), anti IP_3R2 and anti-IP_3R3 treatment (3 nmol per mouse i.c.v.) on mouse motor coordination evaluated in the mouse rota rod test test. ODNs were administered 72, 48 and 24 h prior to the behavioral tests. Vertical lines represent S.E.M. (B) Lack of effect of anti-IP_3R1 (5 nmol per mouse i.c.v.), anti IP_3R2 and anti-IP_3R3 treatment (3 nmol per mouse i.c.v.) on mouse spontaneous mobility and inspection activity evaluated in the mouse hole board test. Amphetamine was administered at a dose of 2 mg kg^{-1} s.c.; ODNs were administered 72, 48 and 24 h prior to the behavioral tests. Vertical lines represent S.E.M.

dODN was observed in terms of detected protein levels (Fig. 6A). Densitometric analysis of all samples revealed that every aODN treatment decreased expression of the corresponding receptors in all cerebral areas investigated (Fig. 6B). Levels of IP_3R1, IP_3R2 and IP_3R3 protein expression returned to normal 7 days after the end of the aODN treatment (data not shown).

Immunoprecipitation experiments also produced similar results. Figure 7 illustrates the reduction of protein expression induced by anti-IP_3R3 in comparison with

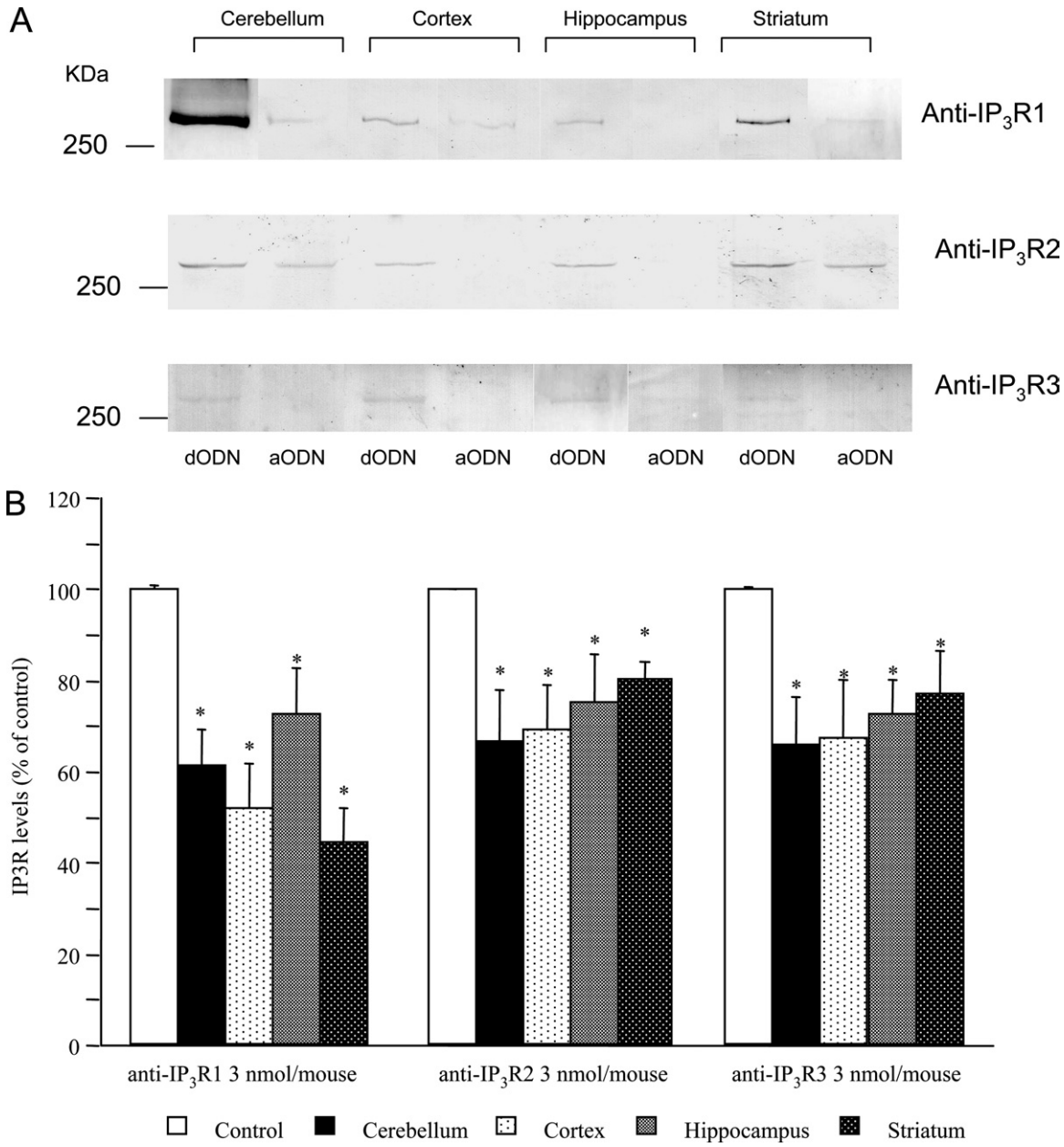

Fig. 6. Reduction of IP_3R1, IP_3R2 and IP_3R3 protein expression in mouse cerebellum, cortex, hippocampus and striatum by aODN treament in comparison with corresponding dODN-treated mice. (A) Samples (30 μg protein/lane) of microsomal fractions of mouse cerebellum, cortex, hippocampus and striatum were resolved on 6% SDS–PAGE, transferred to nitrocellulose and probed with IP_3R1, IP_3R2 or IP_3R3 antibody. (B) Densitometric quantitation of immunoreactive protein expressed relative to control. Data are expressed as means±S.E.M. of band intensities from each of the four groups (n=7 per group). * $P<0.05$ versus control.

dODN-treated mice, taken as an example (Fig. 7A), as well as the densitometric analysis for results obtained in all cerebral areas (Fig. 7B).

Immunoblots were reprobed for a protein considered not regulated as β-actin and no significant density difference was revealed for this protein between samples from the IP_3R1, IP_3R2 and IP_3R3 downregulated brain region (data not shown).

Cross-reactivity of the primary antibodies used was excluded.

DISCUSSION

The present study investigated the role played by type 1, 2 and 3 IP_3R in muscarinic antinociception in a condition of acute thermal nociception in mice. The importance of the receptor-mediated activation of the type 2 and 3 IP_3R isoforms to obtain an increase of the pain threshold was demonstrated.

The specific gene expression knockdown of each of the three IP_3R subtypes was obtained by an oligonucleotide an-

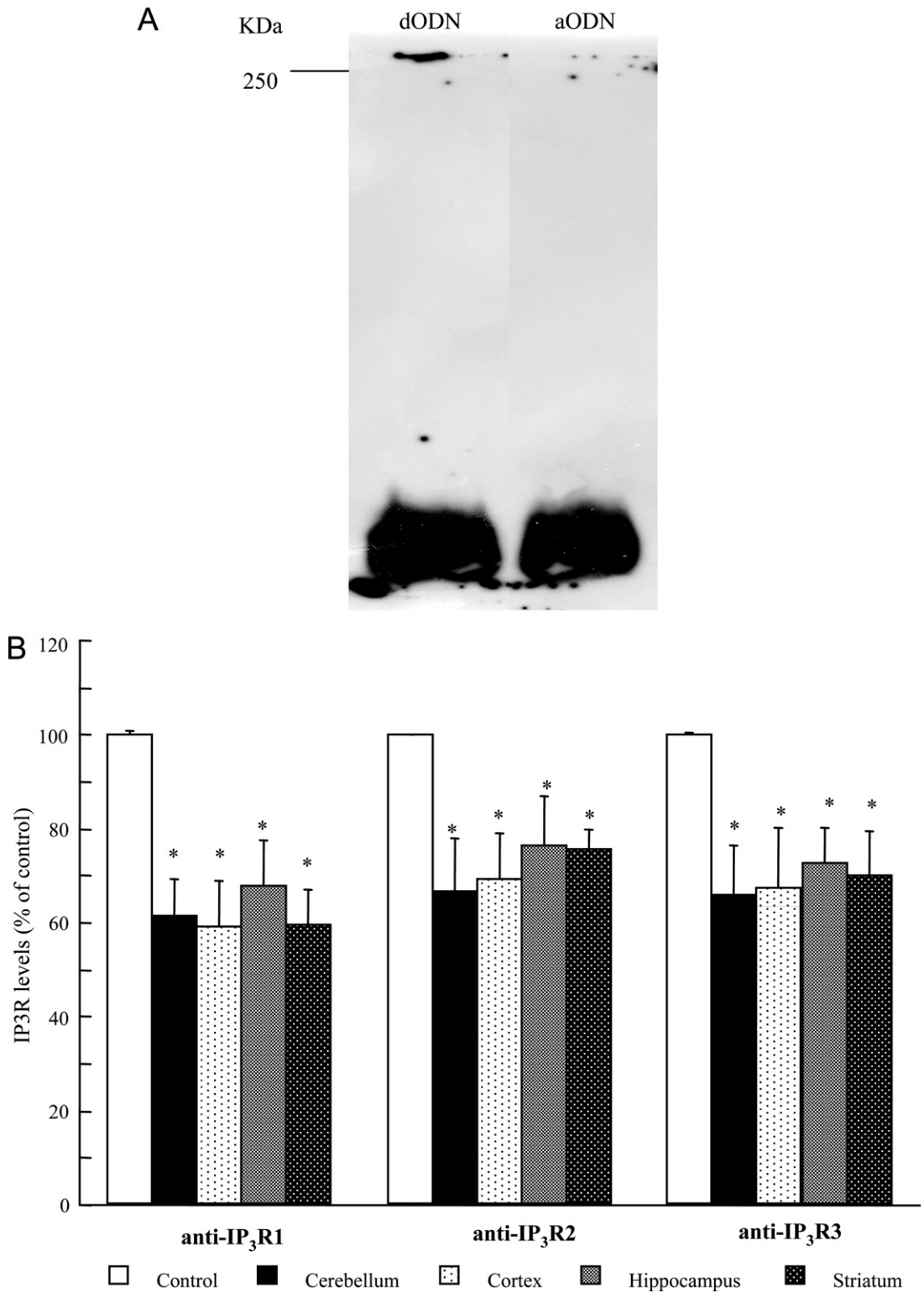

Fig. 7. (A) Reduction of IP_3R3 protein expression in mouse cortex by anti-IP_3R3 treament in comparison with dODN-treated mice. Mouse cortex microsomal membranes were immunoprecipitated with the specific antibody against IP_3R3 and the immunopercipitates, corresponding to 30 μg of original cortex extract, were resolved on 6% SDS–PAGE, transferred to nitrocellulose and probed with IP_3R3 antibody. (B) Densitometric quantitation of immunoreactive protein expressed relative to control. Data are expressed as means±S.E.M. of band intensities from each of the four groups ($n=7$ per group). * $P<0.05$ versus control.

tisense strategy. aODNs are short synthetic DNA segments complementary to sequences of an mRNA target; these specifically bind to targeted mRNA, preventing translation or mediating mRNA cleavage by RNase H and, therefore, transiently inactivate single genes and down-regulating the synthesis of the encoded protein. IP_3R are widely distributed in the central nervous system (CNS) and in the periphery (Vermassen et al., 2004) and, to avoid peripheral effects, the aODNs used were administered directly into the cerebral ventricles.

Administration of an aODN against type 2 IP_3R prevented the antinociception induced by physostigmine and shifted the physostigmine dose–response curve to the right. Similarly, the selective knockdown of the type 3 IP_3R antagonized physostigmine-induced increase of the pain threshold and shifted the dose–response curve of the cholinomimetic drug to the right. Moreover, the inhibition of physostigmine antinociception by anti-IP_3R2 and anti-IP_3R3 antisense oligonucleotides disappeared 7 days after the last i.c.v. injection, indicating a lack of irreversible damage or toxicity on cerebral structures caused by the antisense oligonucleotides. Pretreatment with anti-IP_3R2 and anti-IP_3R3 antisense oligonucleotides in the absence of coadministration of cholinomimetic drugs did not modify the pain threshold, demonstrating the lack of any hyperalgesic effect by the aODN treatment itself. Therefore, the prevention of physostigmine antinociception cannot be attributable to a direct effect on the pain threshold induced by the antisense oligonucleotides. Furthermore, the degenerated oligonucleotide, used as control for the unspecific effects attributable to the administration of nucleic acids irrespective of their specific sequence, did not modify cholinergic antinociception in comparison with naive or saline- and vector-i.c.v. injected mice. This observation ruled out the possibility that the antagonism exerted by the antisense oligonucleotides may have resulted from a sequence-independent action on cerebral structures. This hypothesis was further supported by results of the immunoblotting and immunoprecipitation, where the levels of IP_3R2 and IP_3R3 in microsomes prepared from cerebellum, hippocampus, cortex and striatum of animals treated with the corresponding aODN in comparison with the dODN-treated mice were determined. A selective decrease of IP_3R2 and IP_3R3 protein levels in all cerebral areas investigated was demonstrated, suggesting that the results obtained were related to a selective knockdown of type 2 and 3 IP_3 receptors. Nonspecific effects produced by aODN treatments can, therefore, be excluded. These results suggest that both type 2 and 3 IP_3R subtypes are involved in muscarinic antinociception. These data confirm and extend previous results indicating that supraspinal muscarinic antinociception requires the activation of the M_1 receptor subtype (Ghelardini et al., 2000), which, in turn, activates the PLC–IP_3 pathway, leading to the production of IP_3 and consequent interaction with IP_3R (Galeotti et al., 2003). Furthermore, microdialysis studies demonstrated that the local infusion of carbachol, muscarine and acetylcholine in the rat hippocampus increases IP_3 levels, an effect that was fully prevented by coinfusion with the M_1 antagonist pirenzepine (Minisclou et al., 1994).

The involvement of the M_2 and M_4 muscarinic receptor subtypes in the induction of spinal antinociception was also postulated by using pharmacological antagonists (Gillbert et al., 1989) and by generating M_2 and M_4 muscarinic receptor knockout mice (Gomeza et al., 2001; Chen et al., 2005). Other reports suggest a role of M_2 and M_4 muscarinic receptors in the induction of supraspinal antinociception using muscarinic receptor knockout mice (Duttaroy et al., 2002). The M_2–M_4 receptors are preferentially coupled via G_i proteins to inhibit adenylate cyclase (Caulfield and Birdsall 1998). Expression studies revealed that the cloned M_2 and M_4 receptors also stimulate PLC, although with lower efficiency than the PLC stimulation observed by M_1 or M_3 receptors (Ashkenazi et al., 1987). It is reasonable to suppose that supraspinal muscarinic antinociception, regardless of the receptor subtype involved (M_1 or M_2/M_4), could lead to the activation of the same intracellular metabolic event, the activation of IP_3R.

Although type 2 IP_3R is present in many tissues, high levels are found in spinal cord and glial cells (Sharp et al., 1999). At the subcellular level, it is found in the cell body as well as in processes but is excluded from the nuclear region (Sheppard et al., 1997; Simpson et al., 1997). Type 3 IP_3R is found in the kidney, gastrointestinal tract, pancreatic islets (Nathanson et al., 1994; Taylor et al., 1999; Patel et al., 1999). It is also detected in some neurons, especially in neuron terminals (Sharp et al., 1999). However, the physiological role of these two receptor subtypes in the CNS was not clearly elucidated. The present results provide the first evidence for a role of type 2 and 3 IP_3R in the modulation of pain perception at a supraspinal level.

Type 1 IP_3R is the major neuronal type of IP_3R in the CNS, which is predominantly concentrated in cerebellar Purkinje cells, cerebral cortex, the CA1 region of the hippocampus, basal ganglia and thalamus (Ross et al., 1992; Mikoshiba 1997). The role of IP_3R1 at the CNS level was mainly investigated by means of IP_3R1-deficient mice. Knockout animals showed epilepsy and were deficient in the cerebella long-term depression (Matsumoto and Nagata 1999). Later, a role for the type 1 IP_3R in the modulation of the pain threshold was postulated, because disruption of this receptor prevents morphine-induced antinociception in the mouse (Aoki et al., 2003). Despite this evidence, our observations do not provide evidence for a major role of IP_3R1 in cholinergic antinociception. Pretreatment with an aODN against type 1 IP_3R did not modify the antinociception induced by physostigmine, suggesting a lack of involvement of this receptor subtype in muscarinic antinociception. In DT40 cells stably transfected with M1 muscarinic receptor M1-induced calcium mobilization was unaffected when type 1 IP_3R was deleted. Loss of both type 1 and 2 IP_3R significantly inhibited intracellular Ca^{2+} increase upon carbachol stimulation, whereas Ca^{2+} mobilization was eliminated completely only in cells deficient in all three IP_3R subtypes (Suguwara et al., 1997). The lack of antagonism by the anti-IP_3R1 aODN on cholinergic antinociception as a consequence of inefficient knockdown of the

IP_3R1 protein by the antisense treatment can be ruled out because Western blotting and immunoprecipitation experiments revealed a reduction of the IP_3R1 protein levels not only in the cerebellum, the cerebral area where IP_3R1 is highly expressed, but also in the cortex, hippocampus and striatum of mice pretreated with the highest doses investigated of the anti-IP_3R1 ODN.

Physostigmine, acting as a cholinesterase inhibitor, produces an increase of the ACh levels, which, in turn, can activate both muscarinic and nicotinic receptors. It has been reported that nicotinic antinociception depends on an increase of the intracellular calcium contents. However, the nicotinic component appears not to be involved in the physostigmine-induced increase of pain threshold. Physostigmine antinociception is prevented by atropine and M_1-selective antagonists, as well as by antisense inhibition of M_1 receptors, whereas it is unmodified by nicotinic antagonists, indicating that nicotinic receptors appear not to be involved in the physostigmine-induced increase of the pain threshold (Gillberg et al., 1990; Ghelardini et al., 2000; Yoon et al., 2003).

Furthermore, anti-IP_3R2 and anti-IP_3R3 ODNs under our experimental conditions prevented not only physostigmine antinociception but also the increase of the pain threshold induced by the muscarinic agonist oxotremorine, suggesting that IP_3R activation is necessary to induce muscarinic antinociception.

Receptor-mediated activation of the muscarinic system can induce several side effects. Cholinomimetic drugs can produce the typical cholinergic sympthomatology (tremors, sialorrhea, diarrhea, lacrimation, etc.). Cytosolic Ca^{2+} regulates numerous neuronal functions (Berridge 1998) and, therefore, a variation of intracellular Ca^{2+} content can induce behavioral side effects. aODN effects were tested before the hot plate test was performed to ensure that treatments did not alter the normal locomotor activity, spontaneous mobility and inspection activity of the mice. An influence of the substances used on spontaneous mobility was excluded using the hole board test. Not only modified spontaneous mobility but also altered motor coordination could lead to a misinterpretation of the results obtained. A rota rod test was therefore performed and any alteration of the motor activity induced by aODN administration at the highest doses used was excluded. The results of the rota rod and hole board tests were of particular relevance because it was observed that mice lacking type 1 inositol 1,4,5-trisphosphate receptor showed severe ataxia (Matsumoto et al., 1996) and motor discoordination (Ogura et al., 2001). This discrepancy can be explained by taking into account that the antisense strategy, in comparison with knockout animals, permits, by modulating the degree of inhibition of expression of the target protein, the acquisition of a phenotypic effect without severe toxicity. Moreover, compensatory effects taking place during mouse development, which can mask important phenotypic effects, are avoided. It should also be noted that higher doses of both cholinomimetics and anti-IP_3R could not be investigated because they induced signs of toxicity (tremors, convulsions, etc.) in animals. The induction of toxicity can also be considered an indication not only of the diffusion of these compounds in the brain, but also of the consequent reaching of key targets by using the administration schedule employed in the present study.

Seen as a whole, our data evidence that the selective activation of type 2 and 3 IP_3 receptors is required in the induction of cholinergic supraspinal antinociception in mice in a condition of acute thermal nociception. Furthermore, the lack of a prominent role of the type 1 IP_3 receptor in the increase of pain threshold induced by physostigmine was also demonstrated. An understanding of the cellular events involved in muscarinic antinociception may help develop selective and safe therapeutical approaches for pain relief.

Acknowledgments—This work was supported by grants from MIUR.

REFERENCES

Aoki T, Narita M, Ohnishi O, Mizuo K, Narita M, Yajima Y, Suzuki T (2003) Disruption of the type 1 inositol 1,4,5-trisphosphate receptor gene suppresses the morphine-induced antinociception in the mouse. Neurosci Lett 350:69–72.

Ashkenazi A, Winslow JW, Peralta EG, Peterson GL, Schimerlik MI, Capon DJ, Ramachandran J (1987) An m2 muscarinic receptor subtype coupled to both adenylyl cyclase and phosphoinositide turnover. Science 238:672–675.

Bartolini A, Ghelardini C, Fantetti L, Malcangio M, Malmberg-Aiello P, Giotti A (1992) Role of muscarinic receptor subtypes in central antinociception. Br J Pharmacol 105:77–82.

Berridge MJ (1993) Inositol trisphosphate and calcium signaling. Nature 361:315–325.

Berridge MJ (1998) Neuronal calcium signaling. Neuron 21:13–26.

Caulfield MP, Birdsall NJM (1998) International Union of Pharmacology. XVII. Classification of muscarinic acetylcholine receptors. Pharmacol Rev 50:279–290.

Chen S-R, Wess J, Pan H-L (2005) Functional activity of the M2 and M4 receptor subtypes in the spinal cord studied with muscarinic acetylcholine receptor knockout mice. J Pharmacol Exp Ther 313:765–770.

Duttaroy A, Gomeza J, Gan, J-W, Siddiqui N, Basile AS, Harman WD, Smith PL, Felder CC, Levey AI, Wess J (2002) Evaluation of muscarinic agonist-induced analgesia in muscarinic acetylcholine receptor knockout mice. Mol Pharmacol 62:1084–1093.

Galeotti N, Bartolini A, Ghelardini C (2003) The phospholipase C-IP_3 pathway is involved in muscarinic antinociception. Neuropsychopharmacology 28:888–897.

Ghelardini C, Galeotti N, Bartolini A (2000) Loss of muscarinic antinociception by antisense inhibition of M_1 receptors. Br J Pharmacol 129:1633–1640.

Ghelardini C, Galeotti N, Gualtieri F, Romanelli MN, Bartolini A (1996) S-(-)-ET126, a potent and selective M_1 antagonist in vivo and in vitro. Life Sci 58:991–1000.

Gillberg PG, Hartvig P, Gordh T Jr, Sottile A, Jansson I, Archer T, Post C (1990) Behavioral effects after intrathecal administration of cholinergic receptor agonists in the rat. Psychopharmacology 100: 464–469.

Gillbert PG, Gordh T Jr, Hartvig P, Jansson I, Petterson J, Post C (1989) Characterization of the antinociception induced by intrathecally administered carbachol. Pharmacol Toxicol 64:340–343.

Gomeza J, Zhang L, Kostenis E, Felder CC, Bymaster FP, Brodkin J, Shannon H, Xia B, Duttaroy A, Deng CX, Wess J (2001) Generation and pharmacological analysis of M_2 and M_4 muscarinic receptor knockout mice. Life Sci 68:2457–2466.

Iwamoto ET, Marion L (1993) Characterization of the antinociception produced by intrathecally administered muscarinic agonists in rats. J Pharmacol Exp Ther 266:329–338.

Matsumoto M, Nagata E (1999) Type 1 inositol 1,4,5-trisphosphate receptor knock-out mice: their phenotypes and their meaning in neuroscience and clinical practise. J Mol Med 77:406–411.

Matsumoto M, Nakagawa T, Inoue T, Nagata E, Tanaka K, Takano H, Minowa O, Kuno J, Sakakibara S, Yamada M, Yoneshima H, Miyawaki A, Fukuuchi Y, Furuichi T, Okano H, Mikoshiba K, Noda T (1996) Ataxia and epileptic seizures in mice lacking type 1 inositol 1,4,5-trisphosphate receptor. Nature 379:168–171.

Mikoshiba K (1997) The InsP3 receptor and intracellular Ca^{2+} signaling. Curr Opin Neurobiol 7:339–345.

Minisclou C, Rouquier L, Benavides J, Scatton B, Claustre Y (1994) Muscarinic receptor-mediated increase in extracellular inositol 1,4,5-trisphosphate levels in the rat hippocampus: an in vivo microdyalysis study. J Neurochem 62:557–562.

Naguib M, Yaksh TL (1997) Characterization of muscarinic receptor subtypes that mediate antinociception in the rat spinal cord. Anesth Analg 85:847–853.

Nathanson MH, Fallon MB, Padfield PJ, Maranto AR (1994) Localization of the type 3 inositol 1,4,5-trisphosphate receptor in the Ca^{2+} wave trigger zone of the pancreatic acinar cells. J Biol Chem 269:4693–4696.

Ogura H, Matsumoto M, Mikoshiba K (2001) Motor discoordination in mutant mice heterozygous for the type 1 inositol 1,4,5-trisphosphate receptor. Behav Brain Res 122:215–219.

Patel S, Joseph SK, Thomas AP (1999) Molecular properties of inositol 1,4,5-trisphosphate receptors. Cell Calcium 25:247–264.

Ross CA, Danoff SK, Schell MJ, Snyder SH, Ullrich A (1992) Three additional inositol 1,4,5-triphosphate receptors: molecular cloning and differential localization in rbrain and peripheral tissues. Proc Natl Acad Sci U S A 89:4265–4269.

Sharp AH, Nucifora FC, Blondel O, Sheppard CA, Zhang CY, Snyder SH, Russel JT, Ryugo DK, Ross CA (1999) Differential cellular expression of isoforms of inositol 1,4,5-triphosphate receptors in neurons and glia in brain. J Comp Neurol 406:207–220.

Sheppard CA, Simpson PB, Sharp AH, Nucifora FC, Ross CA, Lange GD, Russel JT (1997) Comparison of type 2 inositol 1,4,5-trisphosphate receptor distribution and subcellular Ca^{2+} release sites that support Ca^{2+} waves in cultured astrocytes. J Neurochem 68: 2317–2327.

Simpson PB, Mehotra S, Lange GD, Russel JT (1997) High density distribution of endoplasmic reticuclum proteins and mitochondria at specialized Ca^{2+} release sites in oligodendrocyte processes. J Biol Chem 272:22654–22661.

Suguwara H, Kuro M, Takada M, Kurosaki T (1997) Genetic evidence for involvement of type 1, type 2 and type 3 inositol 1,4,5-trisphosphate receptors in signal transduction through the B-cell antigen receptor. EMBO J 16:3078–3088.

Taylor CW, Genazzani AA, Morris SA (1999) Expression of inositol trisphosphate receptors. Cell Calcium 26:237–251.

Vaught J, Pelley K, Costa LG, Sether P, Enna SJ (1985) A comparison of the antinociceptive responses to GABA-receptor agonists THIP and baclofen. Neuropharmacology 24:211–216.

Vermassen E, Parys JB, Mauger J-P (2004) Subcellular distribution of the inositol 1,4,5-trisphosphate receptors: functional relevance and molecular determinants. Biol Cell 96:3–17.

Yoon MH, Choi JI, Jeong SW (2003) Antinociception of intrathecal cholinesterase inhibitors and cholinergic receptors in rats. Acta Anaesthesiol Scand 47:1079–108.

APPENDIX

Supplementary data

Supplementary data associated with this article can be found, in the online version, at doi: 10.1016/j.neuroscience.2007.07.049.

(Accepted 4 July 2007)
(Available online 19 August 2007)